Journal of Colloid and Interface Science 329 (2009) 384–389

Contents lists available at ScienceDirect

Journal of Colloid and Interface Science

www.elsevier.com/locate/jcis

On the use of the Stern-layer and the charged-layer formalisms for the interpretation of dielectric and electrokinetic properties of colloidal suspensions

J.J. López-García [a], C. Grosse [b,c], J. Horno [a,*]

[a] Departamento de Física, Universidad de Jaén, Campus Las Lagunillas, Ed. A-3, 23071, Jaén, Spain
[b] Departamento de Física, Universidad Nacional de Tucumán, Av. Independencia 1800, 4000 San Miguel de Tucumán, Argentina
[c] Consejo Nacional de Investigaciones Científicas y Técnicas, Argentina

ARTICLE INFO

Article history:
Received 8 August 2008
Accepted 30 September 2008
Available online 22 October 2008

Keywords:
Standard electrokinetic model
Dynamic Stern-layer model
Charged-layer model
Conductivity increment
Electrophoretic mobility
Dielectric increment

ABSTRACT

The classical description of colloidal suspensions is based on a series of assumptions that constitute the standard electrokinetic model: suspended particles are surrounded by a uniform surface density of fixed charge, the equilibrium ion density coincides with the Gouy–Chapman distribution, and the surface conductivity coincides with the conductivity of the diffuse double layer. Although highly versatile and relatively simple to compute, the classical model often fails to predict crucial experimental trends. Consequently, various attempts have been made to generalize the standard electrokinetic model in order to encompass a broader set of experimental data. Numerical results show that the Stern-layer formalism increases the conductivity and dielectric response but decreases the electrophoretic mobility, while the charged-layer approach leads to electrophoretic mobility values that can actually increase with the surface layer conductivity. Here we compare the predictions of these two surface layer models regarding the conductivity increment, the electrophoretic mobility, and the dielectric increment. We show that for high κa (κ and a being the reciprocal Debye length and the particle radius, respectively) and intermediate electrophoretic mobility values as well as cases when the measured mobility is higher than the maximum value predicted by the standard electrokinetic model, the experimental data can only be interpreted using the charged-layer model.

1. Introduction

The standard model, classically used for the description of the electrokinetic behavior of colloidal suspensions, is based on the following assumptions: suspended particles are surrounded by a uniform surface density of fixed charge, ions can be treated as mathematical points, and the macroscopic permittivity and viscosity values remain valid at the microscopic scale up to the very surface of the particle. With these assumptions, the equilibrium ion density coincides with the Gouy–Chapman distribution, the surface conductivity coincides with the conductivity of the diffuse double layer, and the ζ potential coincides with the equilibrium surface potential.

Accordingly, all the dielectric and electrokinetic properties of the system depend on a series of model parameters (electrolyte concentration, ion valences and diffusion coefficients, fluid permittivity and viscosity, particle size and permittivity) and a single variable: the ζ potential. This makes it possible to determine ζ by means of a single stationary field measurement: either of the DC electrophoretic mobility or of the conductivity increment, since both phenomena are described by the same standard model. A difficulty that often arises is that the values obtained using these two techniques do not coincide with one another [1–3].

This discrepancy seems to reflect a fundamental failure of the standard electrokinetic model: the surface of a colloidal particle might be more complex than assumed by this model. A usual generalization is based on the Stern rather than the Gouy–Chapman ion distribution, assuming that the particle surface is surrounded by a thin layer of ions with surface density determined by adsorption isotherms [4–6] while, outside this layer, the standard model applies. It is further assumed that ions in the surface layer are free to move along the surface while the fluid flow is not allowed. Because of this last assumption, the ζ potential coincides now with the equilibrium potential at the outer boundary of the surface layer. This generalization implies that the surface conductivity includes two parts: the diffuse double layer part (determined by the ζ potential) and the surface layer part (determined by adsorption). Because of this dependence, it is no longer possible to determine the ζ potential from a single stationary field measurement: both DC electrophoretic mobility and conductivity increment measurements are required.

* Corresponding author. Fax: +34 953 212838.
E-mail address: jhorno@ujaen.es (J. Horno).

0021-9797/$ – see front matter
doi:10.1016/j.jcis.2008.09.078

While this seems to solve the compatibility problem between ζ potential values deduced from these two individual measurements [7], a new difficulty arises: the electrophoretic mobility always decreases with the surface layer conductivity. Therefore, this generalization does not help and actually worsens the interpretation of experimental data in those cases when the measured electrophoretic mobility is very high, higher than the theoretical maximum [8]. Still another difficulty arises when the model is extended to the frequency domain [9,10] and the low-frequency dielectric dispersion parameters are compared with experimental data [11]. Quite often, the measured dispersion amplitude is much higher than the theoretical prediction while the characteristic frequency is lower [12–14].

Another type of generalization of the standard model consists in considering that the particle surface might not be perfectly smooth and rigid, which has been modeled as a hairy surface [15,16] or as a thin neutral or charged porous layer [17–24]. The soft charged-layer generalization is also based on the assumption that there is a thin layer surrounding the suspended particle where the equilibrium ion density is not determined by the Gouy–Chapman distribution, while the standard model applies outside its external boundary. The main difference with the Stern-layer model is in that the surface layer is considered to be made both of free ions (mostly counterions) and of the fixed ions that constitute the surface charge. Furthermore, the free ion densities inside the layer are determined by appropriate boundary conditions rather than adsorption isotherms. Finally, the fluid can move along the surface of the particle, only hindered by the presence of the fixed charges and the adhesion condition on its surface. It was recently shown that this generalization of the standard electrokinetic model leads, unlike the Stern-layer generalization, to electrophoretic mobility values that can actually increase with the surface layer conductivity [25].

The purpose of this paper is to compare the predictions of the Stern-layer and the charged-layer generalizations of the standard electrokinetic model for the dielectric and electrokinetic response of dilute suspensions of colloidal spherical particles in AC electric fields. We present numerical results of both surface layer models regarding the conductivity increment, the electrophoretic mobility, and the dielectric increment. We show that for high κa (κ and a being the reciprocal Debye length and the particle radius, respectively) and intermediate electrophoretic mobility values, as well as cases when the measured mobility is higher than the maximum value predicted by the standard electrokinetic model [8], the experimental data can only be interpreted using the charged-layer model.

2. Considered models

The Stern-layer and the charged-layer models considered here as generalizations of the standard model are those proposed by Mangelsdorf and White (M-W) [6] and by López-García, Grosse, and Horno (L-G-H) [25], respectively. In order to simplify the forthcoming discussion and to reduce to a minimum the number of parameters, we consider that the electrolyte solution is binary, univalent, and with equal diffusion coefficient values for the two ionic species. We also consider that the permittivity outside the particle core has a constant value up to its surface and that the ion diffusion coefficient value is the same in the surface layer and in the bulk.

2.1. The dynamic Stern-layer (M-W) model

Since the Stern-layer model proposed by Mangelsdorf and White is fully described in [6] for the DC and in [26] for the AC cases, while a numerical AC solution is given in [10], we will only outline here its main features. It is assumed that the particle bears a fixed surface charge that is located precisely on the core surface, which is surrounded by a surface layer. The "electrokinetic radius" a includes that layer, and the standard electrokinetic equations apply for $r > a$. The surface layer contains free adsorbed ions immersed in a fluid that is not allowed to move.

The equilibrium surface charge density of free ions in the surface layer $\sigma_s^0 = \sigma_{s1}^0 + \sigma_{s2}^0$ is determined by means of adsorption Langevin-type isotherms:

$$\sigma_{sj}^0 = z_j e N_j \frac{\frac{n^\infty}{K_j}\exp\left\{\frac{-z_j e}{k_B T}\left[\psi^0(a) - \frac{\sigma_d^0}{C_2}\right]\right\}}{1 + \sum_{k=1}^{2}\frac{n^\infty}{K_k}\exp\left\{\frac{-z_k e}{k_B T}\left[\psi^0(a) - \frac{\sigma_d^0}{C_2}\right]\right\}}. \quad (1)$$

In this expression, the lower index j refers to the ion type, $z_j e$ is the ion charge ($z_1 = -z_2 = 1$), n^∞ the bulk molar ion density, K_j the dissociation constant (expressed as $K_j = 10^{-\mathrm{pK}_j}$), N_j the maximum surface ion density, $\psi^0(r)$ the equilibrium electric potential, σ_d^0 the surface charge of the diffuse double layer, and C_2 the outer surface layer capacity per unit area.

2.2. The charged-layer (L-G-H) model

The mathematical formulation of the charged-layer model proposed by López-García et al. [25] is identical to that presented earlier for the description of the dielectric and electrokinetic properties of dilute suspensions of soft particles [17,18,23,24]. We will only recall here the main features of this model for sake of completeness and to specify the nomenclature. The model is based on the following assumptions:

(a) The particle is made of a rigid core surrounded by a thin surface layer of thickness $h \approx 1$ nm. The radius of the whole system is a and for $r > a$ the standard electrokinetic equations apply.

(b) The fixed charges of the particle are uniformly distributed inside the surface layer, rather than forming a surface charge on the core surface. This assumption implies that the core is not necessarily a perfectly smooth sphere, that the fixed charges might have a finite size and need not be completely immersed inside the core, and that a hairy surface is a possible reality [15,16].

(c) Both the free ions and the fluid can move inside the surface layer, which seems reasonable since if hydrated ions are allowed to move then water molecules should also be able to move.

(d) Ions are free to move across the external boundary of the surface layer driven by the electric potential and ion concentration gradients, as well as the fluid flow (we do not introduce any adsorption isotherms). Since one of the boundary conditions at $r = a$ is the continuity of the ion concentrations, the ion densities inside the surface layer are close to the densities just outside it.

Note that this model includes a single free parameter λ, related to the resistance exerted by the fixed charges in the surface layer to the fluid flow inside it according to the Debye–Bueche model [27]. The drag coefficient in the soft particle model is defined as [17]

$$\lambda^2 = \frac{\gamma}{\eta},$$

where γ is the force per unit volume and unit fluid velocity while η is the fluid viscosity.

3. Predictions of the models and discussion

In what follows we compare the behavior of the standard electrokinetic model for bare colloids to those of the M-W and of the L-G-H models. We consider different values of the product κa, where

$$\kappa = \sqrt{\frac{2e^2 n^\infty 1000 N_A}{\varepsilon^\infty k_B T}} \quad (2)$$

Table 1
Parameter values used in the calculations except when specified otherwise.

Radius of the core and surface layer	$a = 100 \times 10^{-9}$ m
Thickness of the surface layer	$h = 1 \times 10^{-9}$ m
Absolute permittivity outside the core	$\varepsilon^{\infty} = 78.55 \times 8.85 \times 10^{-12}$ F m^{-1}
Absolute permittivity of the core	$2 \times 8.85 \times 10^{-12}$ F m^{-1}
Viscosity of the suspending medium	$\eta = 0.89 \times 10^{-3}$ poise
Temperature	$T = 298$ K
Number of ion species in the solution	2
Ion valences	$z_1 = -z_2 = 1$
Ion diffusion coefficients	$D_1 = D_2 = 2 \times 10^{-9}$ m^2 s^{-1}
Electrolyte concentration such that	$\kappa a = 30$
Dimensionless surface potential	$y^0(a) = 4$
M-W maximum surface layer charge	$eN_1 = eN_2 = 80$ μC cm^{-2}
Outer surface layer capacity	$C_2 = 130$ μF cm^{-2}

is the reciprocal Debye length, ε^{∞} is the permittivity of the electrolyte solution, and N_A is the Avogadro number, and calculate the different magnitudes as a function of the equilibrium dimensionless surface potential defined as

$$y^0(a) = \frac{e\psi^0(a)}{k_B T}. \tag{3}$$

For the bare particle and the M-W models, this parameter precisely coincides with the dimensionless ζ potential. However, this is not exactly the case for the L-G-H model since the adhesion boundary condition applies at $r = a - h$ rather than $r = a$. Nevertheless, this does not allow us to define the ζ potential in the L-G-H model as the equilibrium potential of the core, since the adhesion condition shifts to $r = a$ when $\lambda \to \infty$ (the ζ potential is an ill-defined parameter in the case of soft particles [19]).

In order to reduce to a minimum the number of parameters we consider, for the L-G-H model, the two extreme cases: $\lambda = 0$ (free fluid flow in the surface layer) and $\lambda \to \infty$ (no fluid flow). Higher values of this parameter up to $\lambda \to \infty$ are certainly meaningful, due to the possible presence of additional features of the particle surface that contribute to further reduce the fluid flow: roughness, hairiness, etc. As for the M-W model, we also consider two extreme cases: $pK_2 \to \infty$ while pK_1 remains finite (no adsorbed co-ions, surface layer fully saturated with counterions) and $pK_1 = pK_2 \to -\infty$ (no adsorbed ions). Actually this last case needs not be calculated since it exactly coincides with the bare particle model. The remaining parameter values are given in Table 1.

Figs. 1–3 represent the dielectric spectrum of the permittivity increment $\Delta\varepsilon(\omega)$ defined as

$$\varepsilon(\omega) = \varepsilon^{\infty}\big[1 + \phi\Delta\varepsilon(\omega)\big], \tag{4}$$

where $\varepsilon(\omega)$ and ε^{∞} are the permittivities of the suspension and of the electrolyte solution while ϕ is the volume fraction of particles, and illustrate its dependence on the surface potential and the product κa. Fig. 1 shows that the L-G-H model leads to roughly a threefold increase of the low-frequency dispersion amplitude as compared to the bare particle model. As expected, the dispersion amplitude is higher the lower the value of λ (the stronger the fluid flow in the surface layer). The M-W model leads to an even higher dispersion amplitude for the surface layer fully saturated with counterions while, as already stated, it leads to the same behavior as the bare particle model in the opposite limit: $pK_j \to -\infty$. The reason for the higher value of the dispersion amplitude predicted by the M-W model with fully saturated surface layer as compared to the L-G-H model is simply due to a higher free counterion surface density (eN_j value in Table 1) [28]. This is verified by the dash and dot line in Fig. 1 that was obtained using the M-W model with pK_j values that lead precisely to the same counterion and co-ion surface densities as in the L-G-H model. As expected, the results of both models coincide when the surface ion densities are the same and there is no fluid flow: $\lambda \to \infty$. Finally,

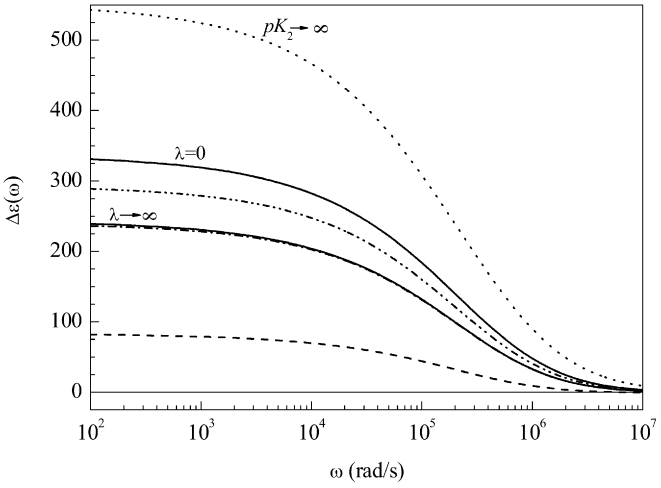

Fig. 1. Permittivity increment, Eq. (4), spectra calculated for $y^0(a) = 4$ and $\kappa a = 30$. Bare particle model and M-W model with $pK_j \to -\infty$, dashed line; M-W model with surface layer saturated with counterions, dotted line; L-G-H model with the indicated λ values, full lines. Remaining parameters given in Table 1. M-W model with pK_j values that lead precisely to the same counterion and co-ion surface densities as the L-G-H model, dash and dot line. Bare particle model with the same fixed charge value as in the L-G-H model (or in the M-W model corresponding to the dash and dot line), dash and double dot line.

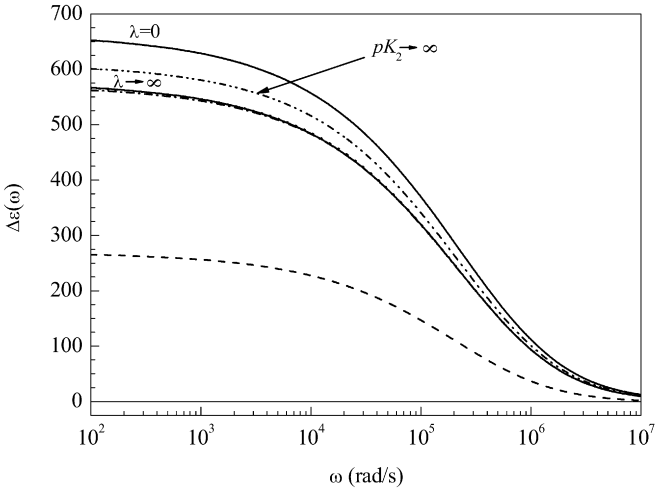

Fig. 2. As for Fig. 1, but calculated for $y^0(a) = 6$ and $\kappa a = 30$.

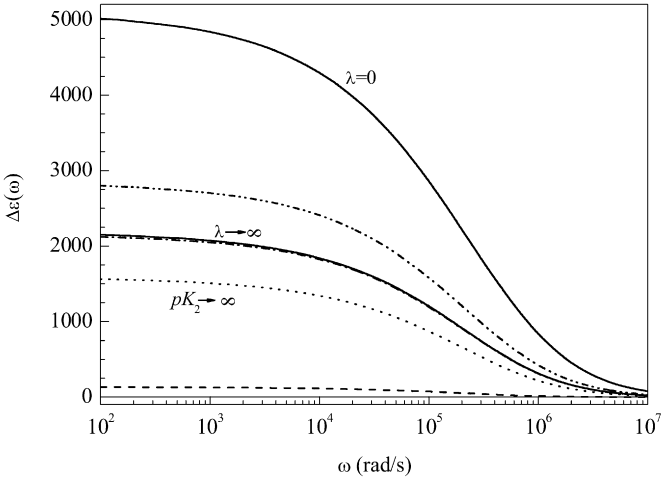

Fig. 3. As for Fig. 1, but calculated for $y^0(a) = 4$ and $\kappa a = 100$.

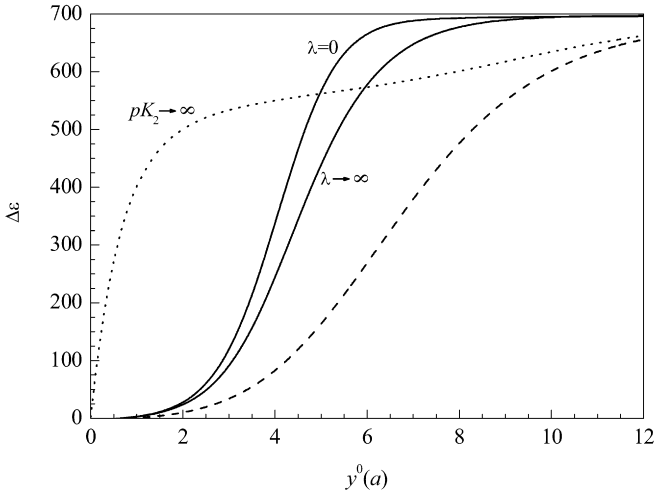

Fig. 4. Dielectric increment, Eq. (5), as a function of the dimensionless surface potential, Eq. (3), calculated for $\kappa a = 30$. Bare particle model and M-W model with $pK_j \to -\infty$, dashed line; M-W model with surface layer saturated with counterions, dotted line; L-G-H model with the indicated λ values, full lines. Remaining parameters given in Table 1.

Fig. 1 also shows the bare particle model behavior calculated using the same value of the fixed charge as in the L-G-H model (or in the M-W model corresponding to the dash and dot line): dash and double dot line. As can be seen, the bare particle model leads, under equal fixed charge rather than equal surface potential condition, to a higher dispersion amplitude than the M-W model, due to a higher surface conductivity (all the free ions are immersed in a fluid that is allowed to flow).

Fig. 2, together with Fig. 1, illustrates the dependence of the dielectric dispersion on the surface potential. While all the considered models lead to higher dispersion amplitude values for higher surface potentials, as expected, the relative differences are smaller than those in Fig. 1 because the dielectric dispersion amplitudes converge to a common value (corresponding to an infinite surface conductivity) for high surface potentials. For this same reason, the dependence of the dispersion amplitude on λ decreases with the surface potential. For $\lambda = 0$, the L-G-H model leads now to a higher dispersion than the M-W model with surface layer fully saturated with counterions. This happens because the ion density in the surface layer increases with the surface potential according to the L-G-H model while, according to the M-W model, it remains at the constant value given in Table 1.

Fig. 3, together with Fig. 1, illustrates the dependence of the dielectric dispersion on the product κa. As expected, all the considered models lead to higher dispersion amplitude values for higher κa since, at constant surface potential and particle size, the ion density in the diffuse double layer increases with κa. Irrespective of the value of λ, the L-G-H model leads now to higher dispersion amplitudes than the M-W model with surface layer fully saturated with counterions. This happens because the ion density in the surface layer increases with κa according to the L-G-H model while, according to the M-W model, it remains at the constant value given in Table 1. Figs. 1 and 3 also show that the dependence of the dispersion amplitude on λ increases with the product κa. This happens because the relative contribution of the conductivity of the surface layer (which depends on the value of λ) to the total surface conductivity increases with κa.

Fig. 4 shows the dielectric increment defined as

$$\Delta\varepsilon = \lim_{\omega \to 0} \Delta\varepsilon(\omega) \tag{5}$$

as a function of the surface potential, calculated for $\kappa a = 30$. The bare particle model shows the well-known behavior corresponding to the amplitude of the low-frequency dielectric dispersion. The L-G-H model leads to much higher dielectric increment values at intermediate surface potentials because of the additional surface conductivity of the surface layer and of the increased surface conductivity of the diffuse layer. This behavior coincides with the often observed experimental behavior [12,13,29–32]. At high surface potential values, the surface layer conductivity tends to infinity while the dielectric increment attains a finite value. The bare particle model tends to this same limiting value for high surface potentials when the diffuse double layer conductivity tends to infinity. As for the M-W model with surface layer fully saturated with counterions, it predicts very high dielectric increments at low surface potentials, since the surface layer conductivity is independent of the surface potential. At high surface potentials, it predicts lower dielectric increment values than the L-G-H model, because the free ion density in the surface layer is lower. Finally, for very high surface potentials, when the diffuse double layer conductivity tends to infinity, it tends to the same limiting value as the L-G-H and the bare particle models.

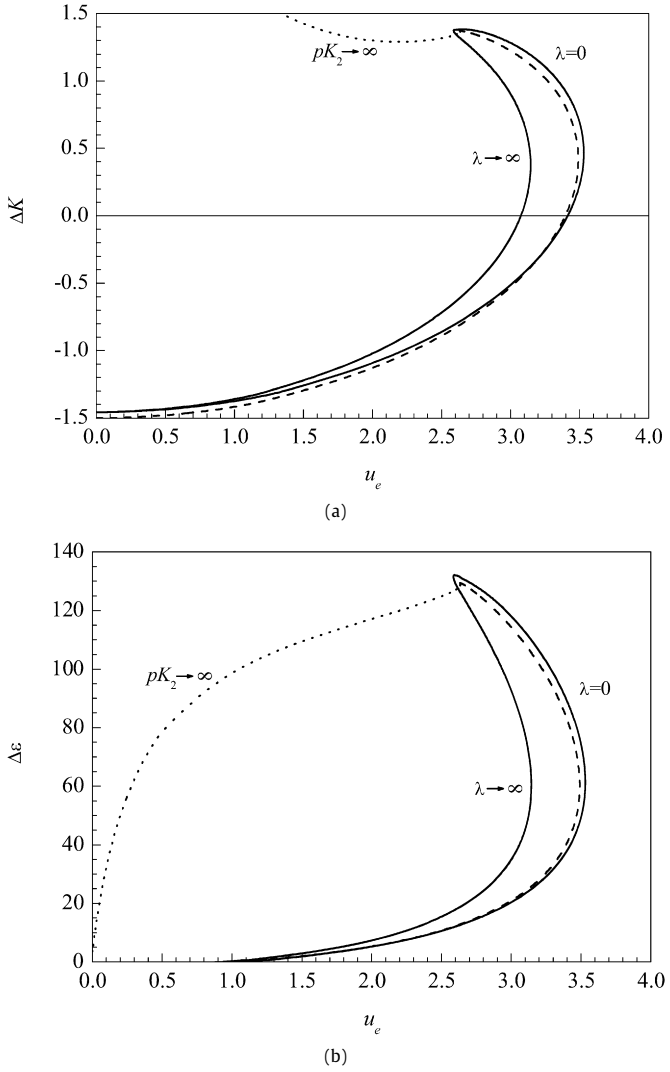

Fig. 5. (a) Conductivity increment, Eq. (6), and (b) dielectric increment, Eq. (5), as functions of the dimensionless electrophoretic mobility, Eq. (7), calculated for $\kappa a = 10$. Bare particle model and M-W model with $pK_j \to -\infty$, dashed line; M-W model with surface layer saturated with counterions, dotted line; L-G-H model with the indicated λ values, full lines. Remaining parameters given in Table 1.

The permittivity spectra calculated in this work, together with the conductivity and electrophoretic mobility values obtained in [25], make it possible to analyze the range of experimental data

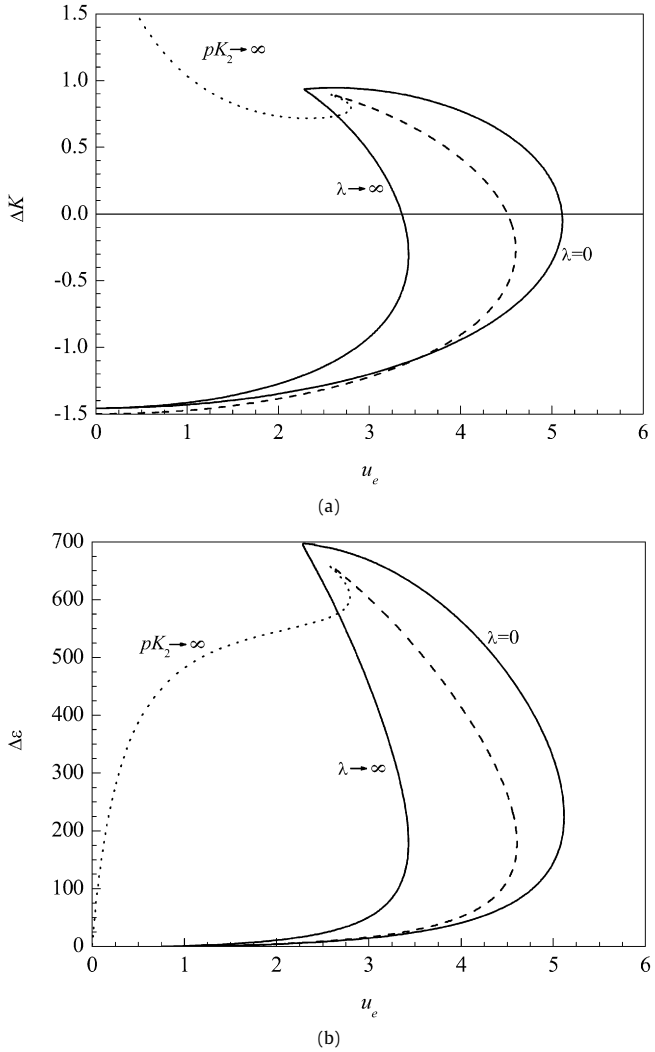

Fig. 6. As for Fig. 5, but calculated for $\kappa a = 30$.

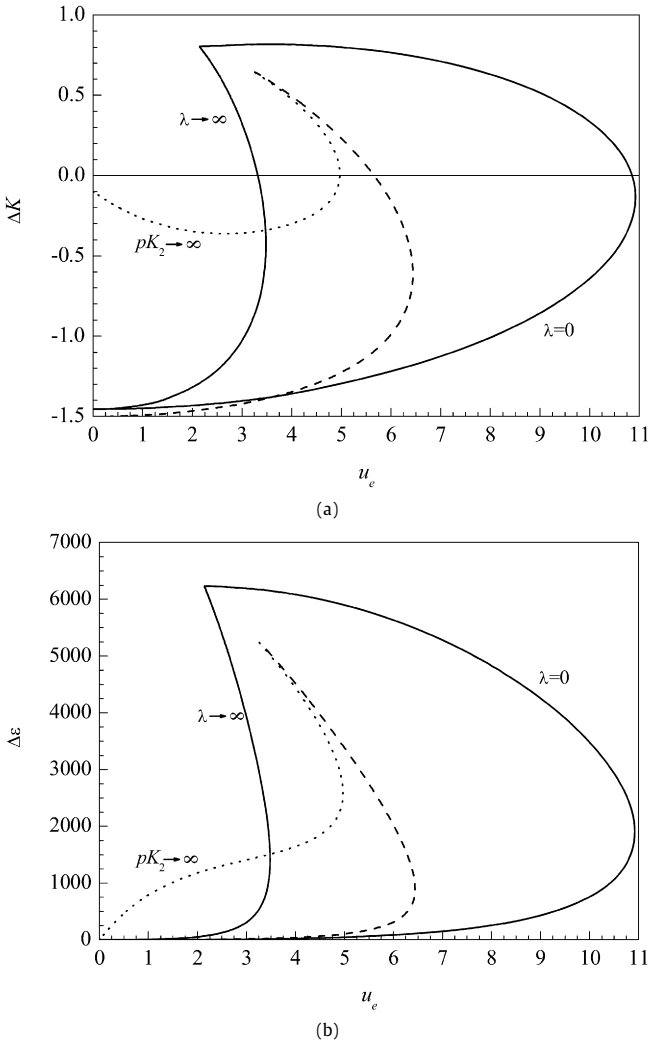

Fig. 7. As for Fig. 5, but calculated for $\kappa a = 100$.

that could be interpreted using the considered models. This is done in Figs. 5–7, which represent the conductivity and dielectric increments as functions of the dimensionless electrophoretic mobility, calculated for three values of the product κa. Each line in these plots corresponds to a given particle–electrolyte solution combination: all the system parameters are kept constant except the fixed surface charge that varies from zero to a very high value. The conductivity increment ΔK is defined as

$$K = K^{\infty}[1 + \phi \Delta K], \tag{6}$$

where K and K^{∞} are the conductivities of the suspension and of the electrolyte solution, while the dimensionless electrophoretic mobility is defined as

$$u_e = \frac{3e\eta}{2\varepsilon^{\infty} k_B T} \frac{v_e}{E}, \tag{7}$$

where v_e is the electrophoretic velocity and E is the applied electric field.

Given a measured electrophoretic mobility value, the bare particle model predicts single conductivity increment and dielectric increment values if the mobility value is low, two possible values if the mobility value is high, and no possible values if the mobility value is very high. As noted in the Introduction, these predicted values are quite often incompatible with the experimental data.

On the contrary, for any measured electrophoretic mobility value, the L-G-H model predicts a continuous range (or two continuous ranges) of possible conductivity increment and dielectric increment values. In Figs. 5–7, these ranges are determined by the intersect of the vertical straight line corresponding to the electrophoretic mobility value, with the area delimited by the $\lambda = 0$ and the $\lambda \to \infty$ curves. For low κa values, the possible conductivity increment and dielectric increment values lie in rather narrow ranges. However, these ranges become extremely broad at high κa and, furthermore, possible solutions appear for electrophoretic mobility data that are higher than the maximum predicted by the bare particle model.

As for the M-W model, it also predicts broad continuous ranges of possible conductivity increment and dielectric increment values for any measured electrophoretic mobility value. In Figs. 5–7, these ranges are determined by the intersect of the vertical straight line corresponding to the electrophoretic mobility value with the area delimited by the dotted curve corresponding to the surface layer fully saturated with counterions and the bare particle model curve. While the M-W model generally predicts even broader ranges than the L-G-H model, there are two important exceptions to this behavior:

(a) High κa and intermediate electrophoretic mobility values. Under these conditions the L-G-H model could make it possible to interpret higher conductivity increment and dielectric increment values than the M-W model.

(b) High electrophoretic mobility. Since the M-W model always predicts lower electrophoretic mobility values than the bare par-

ticle model, any mobility value that surpasses the bare particle model maximum could only be interpreted using the L-G-H model.

4. Conclusion

The generalizations of the standard electrokinetic model proposed by Mangelsdorf and White [6] and by López-García et al. [25] are used to analyze the frequency response of dilute suspensions of spherical colloidal particles to AC electric fields. We compare the predictions of these models regarding the conductivity increment, the electrophoretic mobility, and the dielectric increment.

It should be noted that we are not trying to find out which one of these models better represents the particle–electrolyte solution interface, because actually they complement each other seeking to encompass a broader set of possible particle–electrolyte solution interfaces. Smooth particles with active adsorption sites are certainly best represented by the M-W model, while the L-G-H model is more appropriate for particles that are rough, hairy, or have protruding charged groups.

Our results suggest that measurements of the electrophoretic mobility and of the conductivity and permittivity increments could provide useful information for the characterization of the interface properties in colloidal suspensions. This is specially true for high κa and intermediate electrophoretic mobility values as well as cases when the measured mobility is higher than the maximum value predicted by the standard electrokinetic model since, under these conditions, the experimental data can only be interpreted using the L-G-H model.

Acknowledgments

Financial support for this work by MEC (project FIS2006-4460), FEDER funds, and Junta de Andalucía (project FQM-410), of Spain, and CIUNT (project 26/E312) of Argentina is gratefully acknowledged.

References

[1] R.W. O'Brien, W.T. Perrins, J. Colloid Interface Sci. 99 (1984) 20.
[2] C.F. Zukoski, D.A. Saville, J. Colloid Interface Sci. 107 (1985) 322.
[3] J. Kijlstra, H.P. Van Leeuwen, J. Lyklema, Langmuir 9 (1993) 1625.
[4] T.S. Simonova, V.N. Shilov, Kolloid. Zh. 48 (1986) 370.
[5] C.F. Zukoski, D.A. Saville, J. Colloid Interface Sci. 114 (1986) 32.
[6] C.S. Mangelsdorf, L.R. White, J. Chem. Soc. Faraday Trans. 86 (1990) 2859.
[7] C.F. Zukoski, D.A. Saville, J. Colloid Interface Sci. 114 (1986) 45.
[8] F.J. Arroyo, F. Carrique, A.V. Delgado, J. Colloid Interface Sci. 217 (1999) 411.
[9] L.A. Rosen, J.C. Baygents, D.A. Saville, J. Chem. Phys. 98 (1993) 4183.
[10] C.S. Mangelsdorf, L.R. White, J. Chem. Soc. Faraday Trans. 94 (1998) 2583.
[11] D.E. Dunstan, J. Colloid Interface Sci. 163 (1994) 255.
[12] D.F. Myers, D.A. Saville, J. Colloid Interface Sci. 131 (1989) 461.
[13] L.A. Rosen, D.A. Saville, Langmuir 7 (1991) 36.
[14] A.V. Delgado, F. González-Caballero, R.J. Hunter, L.K. Koopal, J. Lyklema, J. Colloid Interface Sci. 309 (2007) 194.
[15] A.G. Van der Put, B.H. Bijsterbosh, J. Colloid Interface Sci. 92 (1983) 499.
[16] M. Elimalech, C. O'Melia, Colloids Surf. 44 (1990) 165.
[17] J.J. López-García, C. Grosse, J. Horno, J. Colloid Interface Sci. 265 (2003) 327.
[18] J.J. López-García, C. Grosse, J. Horno, J. Colloid Interface Sci. 265 (2003) 341.
[19] H. Ohshima, in: A.T. Hubbard (Ed.), Encyclopedia of Surface and Colloid Science, vol. 2, Dekker, New York, 2002.
[20] J.M. Kleijn, Colloids Surf. 51 (1990) 371.
[21] D.A. Saville, J. Colloid Interface Sci. 222 (2000) 137–145.
[22] H. Ohshima, J. Colloid Interface Sci. 228 (2000) 190.
[23] R.J. Hill, D.A. Saville, W.B. Russel, J. Colloid Interface Sci. 258 (2003) 56.
[24] R.J. Hill, D.A. Saville, W.B. Russel, J. Colloid Interface Sci. 263 (2) (2003) 478.
[25] J.J. López-García, C. Grosse, J. Horno, J. Phys. Chem. B 111 (2007) 8985.
[26] C.S. Mangelsdorf, L.R. White, J. Chem. Soc. Faraday Trans. 94 (1998) 2441.
[27] P. Debye, A. Bueche, J. Chem. Phys. 16 (1948) 573.
[28] F. Carrique, F.J. Arroyo, V.N. Shilov, J. Cuquejo, M.L. Jiménez, A.V. Delgado, J. Chem. Phys. 126 (2007) 104903.
[29] M.M. Springer, A. Korteweg, J. Lyklema, J. Electroanal. Chem. 153 (1983) 55.
[30] K.H. Lim, E.I. Frances, J. Colloid Interface Sci. 110 (1986) 201.
[31] D.E. Dunstan, L.R. White, J. Colloid Interface Sci. 152 (1992) 308.
[32] C. Grosse, M. Tirado, W. Pieper, R. Pottel, J. Colloid Interface Sci. 205 (1998) 26.